

**Dieses Dokument ist eine Zweitveröffentlichung (Verlagsversion) /  
This is a self-archiving document (published version):**

Elena Tsourdi, Juliane Salbach-Hirsch, Martina Rauner, Tilman D. Rachner, Stephanie Möller, Matthias Schnabelrauch, Dieter Scharnweber, Lorenz C. Hofbauer

**Glycosaminoglycans and their sulfate derivatives differentially regulate the viability and gene expression of osteocyte-like cell lines**

**Erstveröffentlichung in / First published in:**

*Journal of Bioactive and Compatible Polymers*. 2014, 29(5), S. 474 - 485 [Zugriff am: 15.08.2019]. SAGE journals. ISSN 1530-8030.

DOI: <https://doi.org/10.1177/0883911514546983>

Diese Version ist verfügbar / This version is available on:


<https://nbn-resolving.org/urn:nbn:de:bsz:14-qucosa2-356895>

„Dieser Beitrag ist mit Zustimmung des Rechteinhabers aufgrund einer (DFGgeförderten) Allianz- bzw. Nationallizenz frei zugänglich.“

This publication is openly accessible with the permission of the copyright owner. The permission is granted within a nationwide license, supported by the German Research Foundation (abbr. in German DFG).

[www.nationallizenzen.de/](http://www.nationallizenzen.de/)

# Glycosaminoglycans and their sulfate derivatives differentially regulate the viability and gene expression of osteocyte-like cell lines

Journal of Bioactive and  
Compatible Polymers  
2014, Vol. 29(5) 474–485  
© The Author(s) 2014  
Reprints and permissions:  
sagepub.co.uk/journalsPermissions.nav  
DOI: 10.1177/0883911514546983  
jbc.sagepub.com  


**Elena Tsourdi<sup>1</sup>, Juliane Salbach-Hirsch<sup>1</sup>, Martina Rauner<sup>1</sup>, Tilman D Rachner<sup>1</sup>, Stephanie Möller<sup>2</sup>, Matthias Schnabelrauch<sup>2</sup>, Dieter Scharnweber<sup>3,4</sup> and Lorenz C Hofbauer<sup>1,4</sup>**

## Abstract

Collagen and glycosaminoglycans, such as hyaluronan and chondroitin sulfate, are the major components of bone extracellular matrix, and extracellular matrix composites are being evaluated for a wide range of clinical applications. The molecular and cellular effects of native and sulfate-modified glycosaminoglycans on osteocytes were investigated as critical regulators of bone remodeling. The effects of glycosaminoglycans on viability, necrosis, apoptosis, and regulation of gene expression were tested in two osteocyte-like cell lines, the murine MLO-Y4 and the rat UMR 106-01 cells. Glycosaminoglycans were non-toxic and incorporated by osteocytic cells. In MLO-Y4 cells, sulfation of glycosaminoglycans led to a significant inhibition of osteocyte apoptosis, 42% inhibition for highly sulfated chondroitin sulfate and 58% for highly sulfated hyaluronan, respectively. Cell proliferation was not affected. While treatment with highly sulfated chondroitin sulfate increased cell viability by 20% compared to the native chondroitin sulfate. In UMR 106-01 cells, treatment with highly sulfated hyaluronan reduced the receptor activator of nuclear factor- $\kappa$ B ligand/osteoprotegerin ratio by 58% compared to the non-sulfated form, whereas highly

<sup>1</sup>Division of Endocrinology, Diabetes and Bone Diseases, Department of Medicine III, TU Dresden Medical Center, Dresden, Germany

<sup>2</sup>Biomaterials Department, INNOVENT e.V., Jena, Germany

<sup>3</sup>Faculty of Mechanical Engineering, Institute of Materials Science, Max Bergmann Center of Biomaterials, TU Dresden, Dresden, Germany

<sup>4</sup>Center for Regenerative Therapies Dresden, Dresden, Germany

## Corresponding author:

Lorenz C Hofbauer, Division of Endocrinology, Diabetes and Bone Diseases, Department of Medicine III, TU Dresden Medical Center, Fetscherstraße 74, 01307 Dresden, Germany.

Email: [lorenz.hofbauer@uniklinikum-dresden.de](mailto:lorenz.hofbauer@uniklinikum-dresden.de)

sulfated chondroitin sulfate led to 60% reduction in the receptor activator of nuclear factor- $\kappa$ B ligand/osteoprotegerin ratio in comparison to the native chondroitin sulfate. The expression of *SOST*, the gene encoding sclerostin, was reduced by 50% and 45% by highly sulfated hyaluronan and chondroitin sulfate, respectively, compared to their native forms. The expression of *BMP-2*, a marker of osteoblast differentiation, was doubled after treatment with the highly sulfated hyaluronan in comparison to its native form. In conclusion, highly sulfated glycosaminoglycans inhibit osteocyte apoptosis *in vitro* and promote an osteoblast-supporting gene expression profile.

### Keywords

Extracellular matrix, bone remodeling, chondroitin sulfate, hyaluronan, osteocyte, gene delivery, gene encoding sclerostin, sulfated glycosaminoglycans, apoptosis, osteoprotegerin

### Introduction

In populations where aging is associated with increased obesity and low physical activity, there is a growing need for biomaterials to replace bone tissue that has been destroyed by degeneration, trauma, tumors, or inflammation, ranging from autologous bone to conventional bone grafts and engineered bone tissue.<sup>1</sup> Because bone implants are characterized by a large variety of their structural composition, their curative potential is also wide.<sup>2,3</sup> It is thus of great significance to define the optimal structural composition of the applied graft material and characterize the cellular response of the host tissue.<sup>4-6</sup> The most promising approach may be to utilize and modify components of the native extracellular matrix (ECM) in order to generate artificial functional matrices (artificial extracellular matrix (aECM)) for the use as bone implants.<sup>7</sup>

The majority of bone is made of the ECM, which can be divided into an inorganic part of hydroxyapatite and an organic part that mainly consists of type I collagen (Coll) with embedded proteoglycans (PGs). PGs consist of a central protein core and peripheral glycosaminoglycan (GAG) chains that have repetitive disaccharide units.<sup>8</sup> The most abundant GAG in bone is chondroitin sulfate (CS), with smaller amounts of hyaluronan (HA) and dermatan sulfate.<sup>9</sup> Because the properties of the GAGs tend to dominate the properties of the entire PG molecule, research has focused on the development of GAG composites to increase implant bioactivity.<sup>10</sup>

Until recently, osteocyte functions were poorly defined, but recent discoveries have underlined the multifactorial profile of these cells in orchestrating bone remodeling by regulating both osteoblast and osteoclast functions.<sup>11</sup> Furthermore, the regulatory role of osteocytes in calcium and phosphate metabolism mainly through the production of fibroblast growth factor 23 (FGF-23)<sup>12</sup> and its mechanosensory role<sup>13</sup> have been highlighted. Taking into account these newly discovered roles as well as the fact that osteocytes make up over 95% of the bone cells in the adult skeleton, the interactions between osteocytes and GAG composites are of key importance. We have recently investigated the effects of the degree of sulfation of GAGs on osteoclast and osteoblast function and signaling pathways and found that highly sulfated GAGs significantly inhibit various functions of bone-resorbing osteoclasts, while stimulating matrix formation in osteoblastic cells.<sup>14-16</sup> However, to our knowledge, there are no studies describing the effects of native or sulfated GAGs on osteocytes.

Here, we synthesized soluble GAG derivatives containing well-defined properties with respect to chain length and sulfation degree and analyzed their effects on osteocyte viability, proliferation, apoptosis, and expression of osteocyte-specific markers. We found that highly sulfated GAGs contributed to the phenotype of healthy, viable, and functional osteocytes as they inhibited osteocyte apoptosis *in vitro* and promoted an osteoblast-supporting gene expression profile.

## Materials and methods

### *Preparation and characterization of GAGs*

Native, high-molecular-weight HA was obtained from Aqua Biochem (Dessau, Germany). CS (a mixture of 70% chondroitin-4-sulfate and 30% chondroitin-6-sulfate) from porcine trachea was purchased from Kraeber (Ellerbek, Germany).

### *GAG modification and synthesis of derivatives*

GAGs were prepared and characterized as previously described.<sup>17–21</sup> In brief, HA sulfates and oversulfated CS derivatives were prepared by sulfation reactions using the tetrabutylammonium salts of native HA and CS. Both highly sulfated hyaluronan (sHA) and highly sulfated chondroitin sulfate (sCS) containing approximately 13 wt% sulfur, corresponding to an average degree of sulfate groups per disaccharide repeating unit ( $DS_S$ ) of 3.1, were sulfated using the  $SO_3^-$ -dimethylformamide (DMF) complex.

Low-molecular-weight HA ( $HA_{LMW}$ ) was prepared by a controlled thermal degradation of the native high-molecular-weight HA as reported.<sup>17–21</sup> The prepared GAG derivatives were characterized spectroscopically by  $^{13}C$ -nuclear magnetic resonance spectroscopy, Fourier transform infrared spectroscopy, and estimation of the sulfur content using a conventional automatic elemental analyzer.<sup>22</sup> The GAG molecular weights were determined by gel-permeation chromatography analysis as described earlier.<sup>17,18</sup>

### *Cell culture of murine and rat osteocytes*

The murine osteocyte-like cell line MLO-Y4 (kindly provided by Dr Lynda Bonewald, Kansas City, MO, USA) was cultured as previously described.<sup>23,24</sup> Briefly, cells were cultured on collagen-coated cell culture flasks (Greiner Bio-One, Frickenhausen, Germany) in alpha-modified essential medium (Biochrom, Berlin, Germany) with 10% fetal calf serum (FCS) (Biochrom), 1% penicillin/streptomycin (Gibco, Darmstadt, Germany), and 2 mM glutamine (Biochrom). Before treatment, cells were placed into serum-free media overnight.

The rat osteocyte-like cell line UMR-106 was kindly provided by Dr Ute Hempel (TU Dresden) and was cultured as previously described.<sup>25</sup> Briefly, cells were cultured on cell culture flasks (Greiner Bio-One) in alpha-modified essential medium (Gibco) with 10% FCS (Biochrom) and 1% penicillin/streptomycin (Gibco). Before treatment, cells were placed into serum-free media overnight.

### *Susceptibility to GAGs*

UMR-106 cells were seeded on glass slides and incubated with fluorescent GAGs for up to 24 h to determine (1) whether osteocytes are susceptible to both the native and the highly sulfated GAGs, (2) where these GAGs localize in the cells, and (3) whether there are kinetic differences. After the incubation period, slides were stained for F-actin and cell nuclei as previously described.<sup>14</sup> Cells cultured without GAGs served as control.

### *Coculture of UMR-106 with RAW264.7 cells*

The murine RAW264.7 cell line is a monocyte cell line with a differentiation potential toward mature osteoclasts. Murine RAW264.7 cells were purchased from American Type Culture

Collection (ATCC) (Wesel, Germany) and cultured on cell culture flasks (Greiner Bio-One) in alpha-modified essential medium (Biochrom) with 10% FCS (PAA), 1% penicillin/streptomycin (Gibco), and 2 mM glutamine (Biochrom). Cells were cultivated up to 85% confluency before being passaged.

UMR-106 cells were plated at 2000 cells/well in 96-well plates and kept for 48 h. Before treatment, cells were placed into serum-free media overnight. Cells were treated with 200  $\mu$ g/mL HA<sub>LMW</sub>, HA, sHA, CS, and sCS for 24 h, at which point the medium was removed and RAW264.7 cells were plated at 4000 cells/well. To initiate osteoclastogenesis, receptor activator of nuclear factor- $\kappa$ B ligand (RANKL) (50 ng/mL, R&D Systems, Minneapolis, MN, USA) was added. Medium was replaced every 2 days, and at the end of culturing, the cells were fixed and stained for tartrate-resistant acid phosphatase (TRAP) using a leukocyte acid phosphatase kit (Sigma Chemical Co., Seelze, Germany) as described previously.<sup>26</sup> Three or more nuclei containing TRAP-positive cells were considered osteoclasts and counted under a microscope.

### **Cell viability**

Cell viability was assessed using a commercial assay (CellTiter-Blue; Promega, Mannheim, Germany) according to the manufacturer's instructions. MLO-Y4 cells were plated at 50,000 cells/well in 96-well plates and kept for 48 h. Before treatment, cells were placed into starving media (0% FCS) overnight. Cells were treated with 200  $\mu$ g/mL HA<sub>LMW</sub>, HA, sHA, CS, and sCS for 24 h, at which point the medium was removed and changed to fresh medium containing the resazurin dye. Viability was determined by the ability of living cells to convert resazurin dye into a fluorescent product within 2–4 h. Fluorescence intensity was quantified using FLUOstar Omega (560<sub>Ex</sub>/590<sub>Em</sub> nm, BMG Labtech).

### **Cell proliferation**

Cell proliferation was assessed using a commercial assay (BrdU; Roche, Grenzach-Wyhlen, Germany) according to the manufacturer's instructions. MLO-Y4 cells were plated at 50,000 cells/well in 96-well plates and kept for 48 h. Before treatment, cells were placed into starving media (0% FCS) overnight. Cells were treated with 200  $\mu$ g/mL HA<sub>LMW</sub>, HA, sHA, CS, and sCS for 24 h while BrdU was added. During this labeling period, the pyrimidine analogue BrdU was incorporated in place of thymidine into the DNA of proliferating cells. After 24 h, the culture medium was removed, and the assay was resumed according to protocol. The reaction product was quantified by measuring the absorbance at 450 nm using FLUOStar Omega (BMG Labtech, Ortenberg, Germany).

### **Cell apoptosis**

Cell apoptosis was assessed using a commercial assay (Caspase-Glo; Promega) according to the manufacturer's instructions. MLO-Y4 cells were plated at 20,000 cells/well in 96-well plates and kept for 48 h. Before treatment, cells were placed into starving media (0% FCS) overnight. Cells were treated with 200  $\mu$ g/mL HA<sub>LMW</sub>, HA, sHA, CS, and sCS for 24 h at which point the medium was removed and the Caspase-Glo reagent was added, resulting in cell lysis, followed by caspase cleavage of the substrate and generation of a glow-type luminescent signal, produced by luciferase. Luminescence was proportional to the amount of caspase activity present and was measured after 60 min using the FLUOStar Omega luminometer.

**Table 1.** Primer sequences used for real-time PCR.

Primer	Sequence 5'-3'
Rat $\beta$ -actin s	5'-GCTACAGCTTCACCACCACA-3'
Rat $\beta$ -actin as	5'-AGGGCAACATAGCACAGCTT-3'
Rat RANKL s	5'-ACCAGCATCAAAATCCCAAG-3'
Rat RANKL as	5'-GGACGCTAATTTCCCTCACCA-3'
Rat OPG s	5'-ACGGTTTGCAAAGATGTCC-3'
Rat OPG as	5'-GTGAGCTGCAGTTGGTGTGT-3'
Rat BMP-2 s	5'-ACATCCACTCCACAAACGAG-3'
Rat BMP-2 as	5'-GTCATTCCACCCACATCAC-3'
Rat GAJ-1 s	5'-GCTCCACTCTCGCCTATGTC-3'
Rat GAJ-1 as	5'-TAGTTCGCCAGTTTTGCTC-3'
Rat SOST s	5'-CAGCTCTCACTAGCCCCCTTG-3'
Rat SOST as	5'-GGGATGATTTCTGTGGCATC-3'

BMP-2: bone morphogenetic protein 2; PCR: polymerase chain reaction; SOST: sclerostin; GAJ-1: gap junction membrane channel protein alpha 1 or connexin 43; RANKL: receptor activator of nuclear factor- $\kappa$ B ligand.

### *RNA isolation, reverse transcriptase and quantitative real-time polymerase chain reaction*

For the detection of messenger RNA (mRNA) expression levels, UMR-106 cells were cultured as described above with or without (control) the addition of 200  $\mu$ g/mL GAGs, respectively. RNA was extracted using a High Pure RNA Isolation Kit from Roche. Then, 500 ng RNA was reverse transcribed using SuperScript<sup>®</sup> II (Invitrogen), and a SYBR<sup>®</sup> Green-based real-time polymerase chain reaction (PCR) under standard conditions was performed. PCR primers were generated with Primer3 and OligoAnalyzer 3.0 software. All applied primer sequences are given in Table 1. The abundance of mRNA levels was calculated using the  $\Delta\Delta$ CT method<sup>27</sup> and is presented as increases relative to an untreated or undifferentiated control.

### *Statistical analyses*

All experiments were performed at least in triplicates and evaluated using one-way analysis of variance (ANOVA). Student's *t*-test was performed to compare native GAGs with modified GAGs. All results are presented as the mean  $\pm$  standard deviation (SD); *p* values <0.05 were considered statistically significant.

## **Results and discussion**

### *Osteocyte susceptibility to differentially sulfated GAGs*

UMR-106 and MLO-Y4 cells ingested both native and sulfated HA (Figure 1(a)—data for MLO-Y4 and data for UMR-106 are not shown). After 24 h, GAGs were detected in vesicles in the perinuclear region. This localization was observed earlier for the shorter, highly sulfated HA, where the first vesicles were found after 1 h, whereas vesicles of native HA did not appear before 6 h. This effect has been corroborated by the interactions between human mesenchymal stromal cells (MSC) and sulfated HA-containing collagen matrices where an upregulation of endocytic proteins was noted.<sup>28</sup> The fact that both forms of HA appeared intracellularly excludes the possibility that GAG

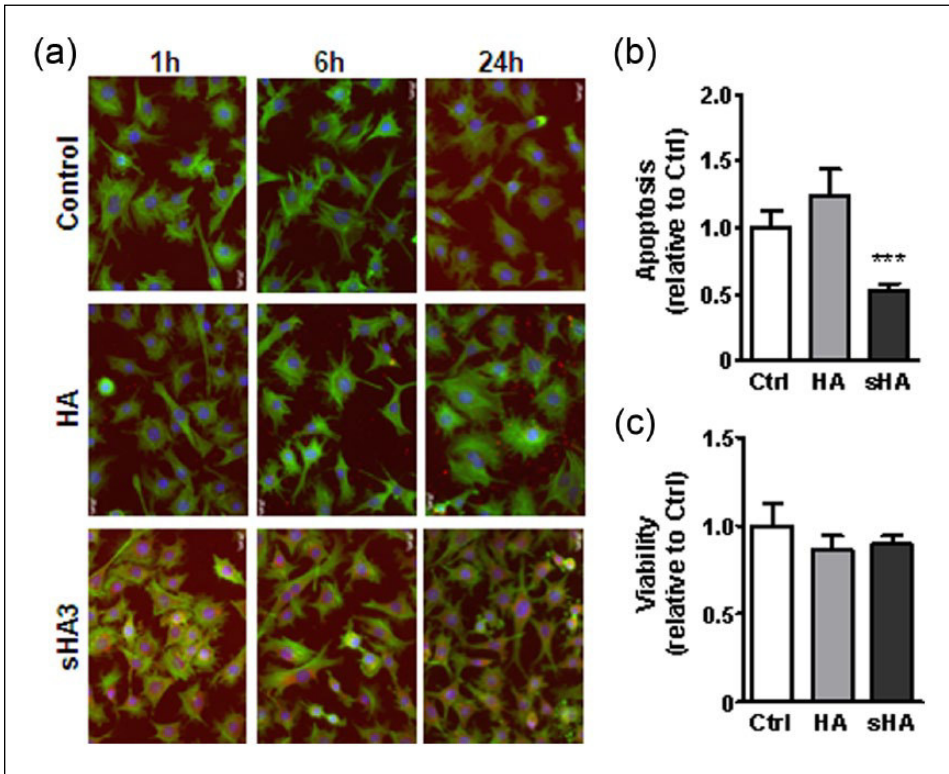


**Figure 1.** (a) Osteocytes are susceptible to native and sulfated fluorescent GAGs. MLO-Y4 and UMR-106 cells seeded on glass slides were exposed to red-fluorescent native hyaluronan (HA) or sulfated HA (sHA) for 1, 6, or 24 h. Untreated cells served as controls (Ctrl). Subsequently, slides were stained for F-actin (green) and cell nuclei (blue) and analyzed using digital microscopy. A representative image of three replicates is shown (magnification 400 $\times$ ), data shown for MLO-Y4. (b) Sulfated HA modulates apoptosis of osteocytes. Cell apoptosis was assessed on MLO-Y4 cells by a luminescence assay after 1 h. Luminescence was proportional to the amount of caspase activity. (c) Sulfated HA has no significant effect on viability of osteocytes. Cell viability was assessed on MLO-Y4 cells using a fluorescence assay after 2–4 h using resazurin dye. Values represent the mean  $\pm$  standard deviation (SD) of  $n=6-10$  measurements.

\* $p < 0.05$ , \*\* $p < 0.01$ , and \*\*\* $p < 0.001$ ; Student's *t*-test versus treatment with native GAG.

sulfation results in impaired uptake that could affect all subsequent effects. A potential limitation of our study was the fact that the immunofluorescence experiments were conducted using only native and highly sulfated HA and not CS.

### Sulfation of GAGs reduces osteocyte apoptosis

After establishing GAG localization in the perinuclear region of osteocytes, we examined the effect of GAG treatment on osteocyte apoptosis. Treatment for 24 h with highly sulfated GAGs at a concentration of 200  $\mu\text{g}/\text{mL}$  led to a significant reduction in osteocyte apoptosis in MLO-Y4 cells. Treatment with sHA led to a 58% decrease in apoptosis when compared to HA ( $p < 0.001$ ) (Figure 1(b)), whereas sCS reduced apoptosis by 42% when compared to its native product ( $p < 0.01$ ) (Figure 2). Native HA and CS tended to increase osteocyte apoptosis, but these results were not statistically significant. HA<sub>LMW</sub> had no significant effects on osteocyte apoptosis (data not shown).

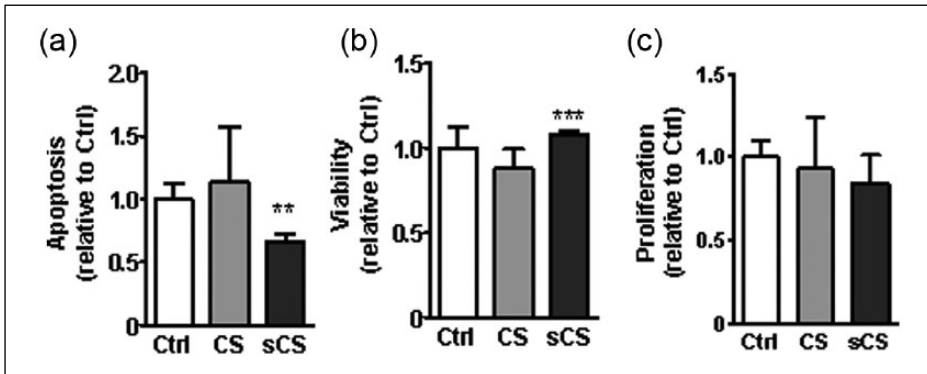


**Figure 2.** Sulfated CS modulates apoptosis and viability of osteocytes but has a neutral effect on osteocyte proliferation. (a) Cell apoptosis was assessed on MLO-Y4 cells by a luminescence assay after 1 h. Luminescence was proportional to the amount of caspase activity. (b) Cell viability was assessed on MLO-Y4 cells using a fluorescence assay after 2–4 h using resazurin dye. (c) Cell proliferation was assessed on MLO-Y4 cells using an absorbance assay measuring the incorporation of the pyrimidine analogue into the DNA of proliferating cells after 24 h. Values represent the mean  $\pm$  SD of  $n=6-10$  measurements. Ctrl: control; CS: native chondroitin sulfate; sCS: highly sulfated chondroitin sulfate; SD: standard deviation. \* $p < 0.05$ , \*\* $p < 0.01$ , and \*\*\* $p < 0.001$ ; Student's *t*-test versus treatment with native GAG.

### Sulfation of GAGs differentially regulate osteocyte viability, but not proliferation

The effects of highly sulfated GAGs on osteocyte viability and proliferation were assessed next. Neither native nor highly sulfated HA had any significant effect on osteocyte viability (Figure 1(c)) and HA<sub>LMW</sub> had also no significant effect on osteocyte apoptosis (data not shown). Treatment with sCS increased cell viability by 20% compared to its native product ( $p < 0.001$ ) (Figure 2). Treatment with sHA did not significantly affect cell viability. Our data also indicate that treatment with GAGs both in their native and their highly sulfated form had a neutral effect on osteocyte proliferation (Figure 2(c), data for CS shown).

In summary, we observed an anti-apoptotic effect of highly sulfated HA and CS on osteocytes. Furthermore, treatment of osteocytes with sulfated CS, but not native GAGs, led to an enhancement of cell viability, whereas all GAGs had no significant effect on cell proliferation. Of note, treatment with HA<sub>LMW</sub> had no significant effect on osteocyte apoptosis and viability. It can thus be concluded that the degree of sulfation, rather than the monosaccharide composition of GAGs, determines biological functions. GAG sulfation inhibited apoptosis and enhanced viability. Thus, highly sulfated GAGs would represent suitable candidates for preclinical testing in appropriate animal models. We have already shown that GAG sulfation led to a significant inhibition of osteoclast differentiation and resorption<sup>14</sup> and supported osteoblast functions.<sup>16</sup> Extrapolation of our findings from *in vitro* to the *in vivo* situation suggests that sulfated GAGs could contribute to the phenotype of healthy, viable, and functional osteocytes, thus supporting our previous results on osteoclasts and osteoblasts. However, this needs to be formally tested in appropriate *in vivo* models.

### GAG sulfation affects the expression of osteocytic genes

Since UMR-106 cells express genes such as *sclerostin*, *RANKL*, and *connexin-43*, we used these cells as a model to assess the effects of GAGs on the regulation of osteocytic gene expression. Exposure of UMR-106 cells to native GAGs resulted in a consistent downregulation of *RANKL*, which promotes osteoclastogenesis. Using a concentration of 200  $\mu\text{g}/\text{mL}$ , we found that sHA



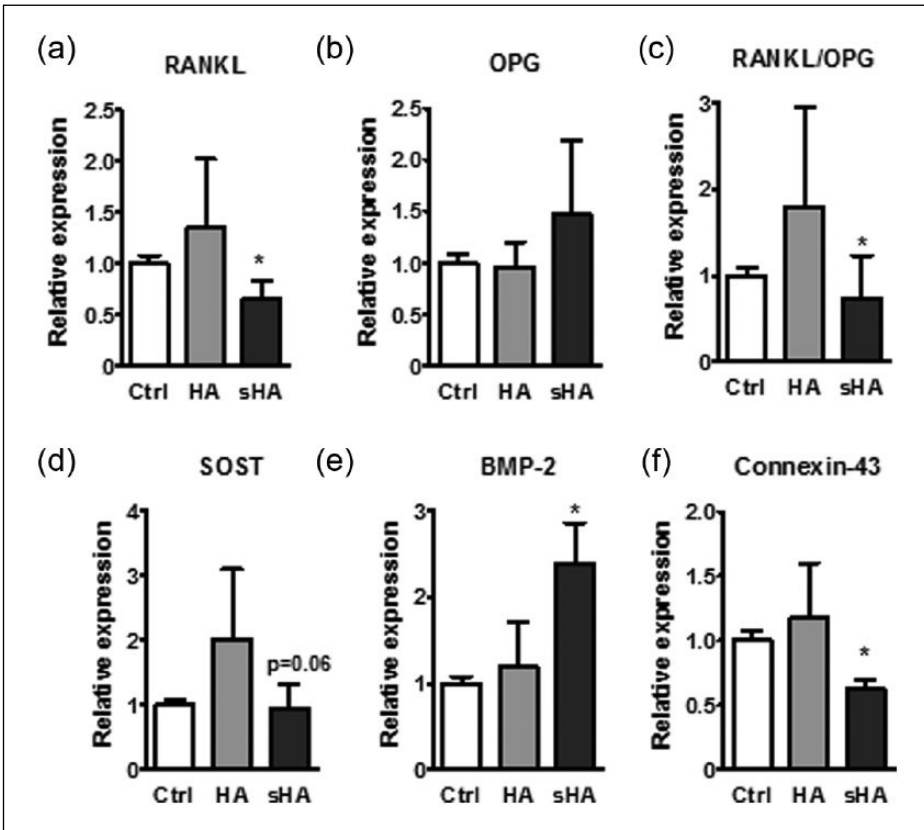


**Figure 3.** Regulation of osteocyte-specific markers through HA and sHA. (a)–(f) Quantitative real-time PCR analysis of RANKL, OPG, SOST, BMP-2, and GAJ-1 expression levels of UMR-106 cells exposed to 200  $\mu\text{g}/\text{mL}$  of HA and sHA. All values represent the normalized mean  $\pm$  SD of  $n = 6$ . Ctrl: control; HA: native hyaluronan; sHA: highly sulfated hyaluronan; RANKL: receptor activator of nuclear factor- $\kappa\text{B}$  ligand; OPG: osteoprotegerin; SOST: sclerostin; BMP-2: bone morphogenetic protein 2; GAJ-1: gap junction membrane channel protein alpha 1 or connexin 43; SD: standard deviation; PCR: polymerase chain reaction. \* $p < 0.05$ , \*\* $p < 0.01$ , and \*\*\* $p < 0.001$ ; Student's  $t$ -test versus treatment with native GAG.

downregulated the expression of *RANKL* by 50% in comparison with its native form ( $p < 0.05$ ) (Figure 3(a)), whereas treatment with sCS did not significantly influence *RANKL* expression (Figure 4(a)). Treatment with GAGs had a neutral effect on the expression of *osteoprotegerin* (OPG) (Figures 3(b) and 4(b)), but led to a significant downregulation of the RANKL/OPG ratio. In particular, sHA reduced the RANKL/OPG ratio by 58% in comparison with its native form (Figure 3(c)) ( $p < 0.05$ ), an effect also seen for sCS (Figure 4(c)). Furthermore, the expression of *SOST*, the gene encoding sclerostin, was reduced by both highly sulfated GAGs when compared to their native forms ( $-50\%$ ,  $p = 0.06$  for HA and  $-45\%$ ,  $p < 0.05$  for CS, respectively) (Figure 4(c) and (d)).

By contrast, the expression of genes enhancing osteoblast and osteocyte differentiation, such as *BMP-2*, was found to be upregulated twofold by highly sulfated HA as compared to its native form ( $p < 0.05$ ) (Figure 3(e)). Treatment with sCS did not lead to a significant increase in *BMP-2* expression (Figure 4(e)). The expression of *GAJ-1*, the gene encoding connexin 43, an important gap junction protein in osteocytes, was downregulated by sHA as compared to its native form ( $p < 0.05$ )

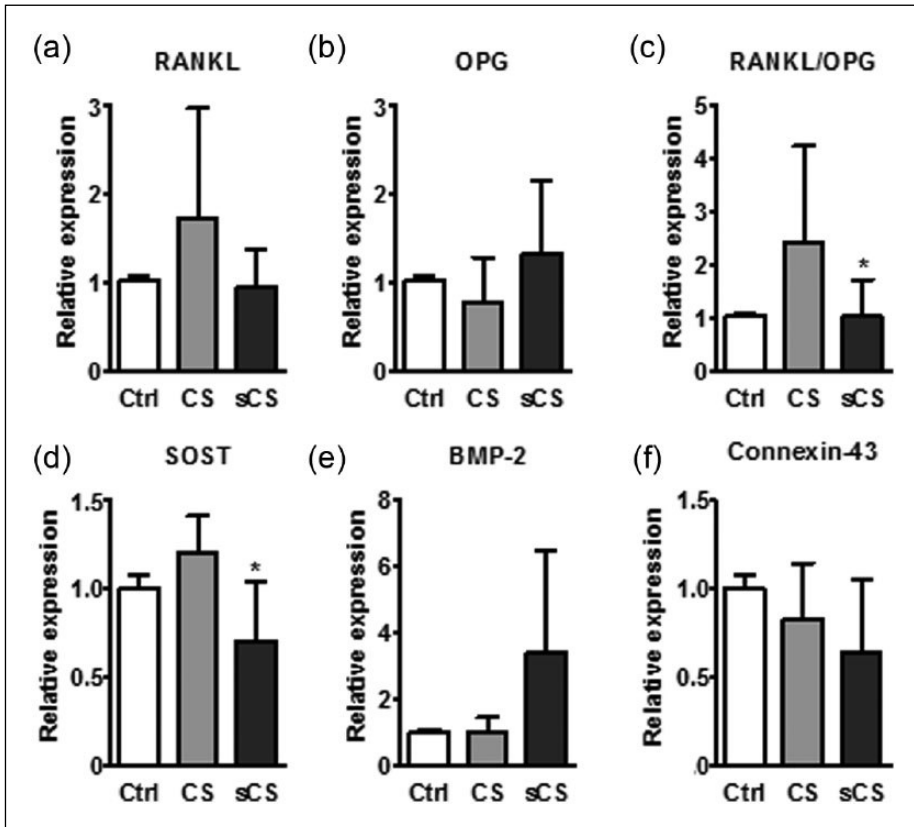


**Figure 4.** Regulation of osteocyte-specific markers through CS and sCS. (a)–(f) Quantitative real-time PCR analysis of RANKL, OPG, SOST, BMP-2, and GAJ-1 expression levels of UMR-106 cells exposed to 200  $\mu\text{g/mL}$  of CS and sCS. All values represent the normalized mean  $\pm$  SD of  $n=6$ .

Ctrl: control; CS: native chondroitin sulfate; sCS: highly sulfated chondroitin sulfate; RANKL: receptor activator of nuclear factor- $\kappa$ B ligand; OPG: osteoprotegerin; SOST: sclerostin; BMP-2: bone morphogenetic protein 2; GAJ-1: gap junction membrane channel protein alpha 1 or connexin 43; SD: standard deviation; PCR: polymerase chain reaction. \* $p < 0.05$ , \*\* $p < 0.01$ , and \*\*\* $p < 0.001$ ; Student's  $t$ -test versus treatment with native GAG.

(Figure 3(f)). Neither CS nor its sulfated form influenced *GAJ-1* expression (Figure 4(f)). HA<sub>LMW</sub> had no significant effects on the expression of osteocyte markers (data not shown).

When considering osteocyte gene expression, our data indicated that sHA significantly reduces the expression of *RANKL* and both highly sulfated HA and CS downregulate the *RANKL/OPG* ratio. In bone homeostasis, the expression of *RANKL* and *OPG* is balanced resulting in physiological bone remodeling. An overexpression of *RANKL* is observed in estrogen deficiency,<sup>29</sup> systemic glucocorticoid exposure, and active inflammatory processes in rheumatoid arthritis,<sup>30</sup> skeletal malignancies such as multiple myeloma,<sup>31</sup> and bone metastases.<sup>32</sup> All these conditions are characterized by excessive bone loss, implying that the upregulation of the *RANKL/OPG* ratio promotes excessive bone resorption. Thus, it may be envisaged that treatment of osteocytes with highly sulfated GAGs suppresses their paracrine ability to support osteoclast differentiation and resorption.

Furthermore, treatment with highly sulfated GAGs led to a significant reduction in *SOST* and regulated *BMP-2* as well as *GAJ-1*, the gene encoding connexin 43. To this end, inhibition of

sclerostin and upregulation of connexin 43 and BMP-2 through GAGs could contribute to the phenotype of viable and functional osteocytes and osteoblasts.

### Coculture of UMR-106 with RAW264.7 cells

After having found a considerable regulation of the RANKL/OPG ratio by highly sulfated GAGs, we performed cocultures of osteocytes/osteoclasts. Treatment with native HA and HA<sub>LMW</sub> led to an inhibition of osteoclastogenesis by 40%, whereas highly sulfated HA and both forms of CS tended to enhance osteoclastogenesis; nevertheless, these results did not reach a level of statistical significance.

Despite its strength, our study has potential limitations. We observed a regulation of RANKL but not OPG through GAGs, and in contrast to our expectations, it was the native and not the sulfated form of HA that led to an inhibition of osteoclastogenesis. We hypothesize that the addition of RANKL in a concentration of 50 ng/mL in a latter phase of the coculture might have dominated the effect of GAGs on osteocytes or alternatively that RANKL directly bound to OPG influencing the results. Another limitation is the fact that both cell lines used possess at the most an osteocyte-like phenotype, in that the MLO-Y4 cells represent the osteocyte morphology and the UMR-106 cells represent the osteocyte gene expression, while neither cell line combines both characteristics as primary human osteocytes would. In this context, one can only hypothesize as to whether the results gained by experiments using osteocyte-like cell lines can be extrapolated to the *in vivo* environment.

## Conclusion

Based on our data, GAGs inhibit osteocyte apoptosis and promote osteocyte viability while maintaining a physiological RANKL/OPG ratio. These results are in accordance with the pro-osteoblastic and anti-osteoclastic effects of sulfated GAGs that we previously reported. The present data confirm these functions on osteocytes, which represent the most abundant cell type and indicate a promising potential as a component of diverse biomaterials. However, our conclusions at this time are based only on *in vitro* data and require *in vivo* validation.

## Acknowledgements

We thank Dr Lynda F. Bonewald for providing the MLO-Y4 cells and Dr Ute Hempel for providing the UMR-106 cells. We thank Nicole Pacyna and Claudia Richter for their excellent technical assistance.

## Declaration of conflicting interests

The authors declared no potential conflicts of interest with respect to the research, authorship, and/or publication of this article.

## Funding

This study was supported by grants from Deutsche Forschungsgemeinschaft Transregio 67 (subproject A2, A3, and B2).

## References

1. Amiri AR, Laurencin CT and Nukavarapu SP. Bone tissue engineering: recent advances and challenges. *Crit Rev Biomed Eng* 2012; 40(5): 363–408.
2. Dinopoulos H, Dimitriou R and Giannoudis PV. Bone grafts: what are the options? *Surgeon* 2012; 10(4): 230–239.
3. Fini M, Giavaresi G, Torricelli P, et al. Osteoporosis and biomaterial osteointegration. *Biomed Pharmacother* 2004; 58(9): 487–493.
4. Zhang H and Hiu J. Electrospun poly(lactic-co-glycolic acid)/wool keratin fibrous composite scaffolds potential for bone tissue engineering

- applications. *J Bioact Compat Pol* 2013; 28(2): 141–153.
5. Mota C, Puppi D, Dinucci D, et al. Additive manufacturing of star poly( $\epsilon$ -caprolactone) wet-spun scaffolds for bone tissue engineering applications. *J Bioact Compat Pol* 2013; 28(4): 320–340.
  6. Yan LP, Salgado AJ, Oliveira JM, et al. De novo bone formation on macro/microporous silk and silk/nano-sized calcium phosphate scaffolds. *J Bioact Compat Pol* 2013; 28(5): 439–452.
  7. Li QL, Huang N, Chen JL, et al. An extracellular matrix-like surface modification on titanium improves implant endothelialization through the reduction of platelet adhesion and the capture of endothelial progenitor cells. *J Bioact Compat Pol* 2013; 28(1): 33–49.
  8. Robey PG and Boskey AL. The composition of bone. In: Rosen CJ (ed.), *Primer on the metabolic bone diseases and disorders of mineral metabolism*. Hoboken, NJ: John Wiley & Sons, Inc., 2009, pp. 74–79.
  9. Salbach J, Rachner TD, Rauner M, et al. Regenerative potential of glycosaminoglycans for skin and bone. *J Mol Med* 2012; 90(6): 625–635.
  10. Catini C and Gheri G. The GAGs of the bone: a study of human calva. *Arch Ital Anat Embriol* 1990; 95(3–4): 237–240.
  11. Bonewald LF. The amazing osteocyte. *J Bone Miner Res* 2011; 26(2): 229–238.
  12. Feng JQ, Ward LM, Liu S, et al. Loss of DMP1 causes rickets and osteomalacia and identifies a role for osteocytes in mineral metabolism. *Nat Genet* 2006; 38(11): 1310–1315.
  13. Klein-Nulend J, van der Plas A, Semeins CM, et al. Sensitivity of osteocytes to biomechanical stress in vitro. *Faseb J* 1995; 9(5): 441–445.
  14. Salbach J, Kliemt S, Rauner M, et al. The effect of the degree of sulfation of glycosaminoglycans on osteoclast function and signaling pathways. *Biomaterials* 2012; 33(33): 8418–8429.
  15. Salbach-Hirsch J, Kraemer J, Rauner M, et al. The promotion of osteoclastogenesis by sulfated hyaluronan through interference with osteoprotegerin and receptor activator of NF- $\kappa$ B ligand/osteoprotegerin complex formation. *Biomaterials* 2013; 34(31): 7653–7661.
  16. Salbach-Hirsch J, Ziegler N, Thiele S, et al. Sulfated glycosaminoglycans support osteoblast functions and concurrently suppress osteoclasts. *J Cell Biochem* 2014; 115(6): 1101–1111.
  17. Kunze R, Rösler M, Möller S, et al. Sulfated hyaluronan derivatives reduce the proliferation rate of primary rat calvarial osteoblasts. *Glycoconj J* 2010; 27(1): 151–158.
  18. Hintze V, Moeller S, Schnabelrauch M, et al. Modifications of hyaluronan influence the interaction with human bone morphogenetic protein-4 (hBMP-4). *Biomacromolecules* 2009; 10(12): 3290–3297.
  19. Van der Smissen A, Hintze V, Scharnweber D, et al. Growth promoting substrates for human dermal fibroblasts provided by artificial extracellular matrices composed of collagen I and sulfated glycosaminoglycans. *Biomaterials* 2011; 32(34): 8938–8946.
  20. Hempel U, Hintze V, Möller S, et al. Artificial extracellular matrices composed of collagen I and sulfated hyaluronan with adsorbed transforming growth factor  $\beta$ 1 promote collagen synthesis of human mesenchymal stromal cells. *Acta Biomater* 2012; 8(2): 659–666.
  21. Bothner H and Wik O. Rheology of hyaluronate. *Acta Otolaryngol Suppl* 1987; 442: 25–30.
  22. Volpi Mucci A and Schenetti L. Stability studies of chondroitin sulfate. *Carbohydr Res* 1999; 315(3–4): 345–349.
  23. Kato Y, Windle JJ, Koop BA, et al. Establishment of an osteocyte-like cell line, MLO-Y4. *J Bone Miner Res* 1997; 12(12): 2014–2023.
  24. Thiele S, Ziegler N, Tsourdi E, et al. Selective glucocorticoid receptor modulation maintains bone mineral density in mice. *J Bone Miner Res* 2012; 27(11): 2242–2250.
  25. Partridge NC, Alcorn D, Michelangeli VP, et al. Morphological and biochemical characterization of four clonal osteogenic sarcoma cell lines of rat origin. *Cancer Res* 1993; 43(9): 4308–4314.
  26. Oreffo RO, Marshall GJ, Kirchen M, et al. Characterization of a cell line derived from a human giant cell tumor that stimulates osteoclastic bone resorption. *Clin Orthop Relat Res* 1993; 296: 229–241.
  27. Livak KJ and Schmittgen TD. Analysis of relative gene expression data using real-time quantitative PCR and the 2(-Delta Delta C(T)). *Methods* 2001; 25(4): 402–408.
  28. Kliemt S, Lange C, Otto W, et al. Sulfated hyaluronan containing matrices enhance cell-matrix-interaction, endocytosis, and osteogenic

- differentiation of human mesenchymal stromal cells. *J Proteome Res* 2013; 12(1): 378–389.
29. Eghbali-Fatourehchi G, Khosla S, Sanyal A, et al. Role of RANK ligand in mediating increased bone resorption in early postmenopausal women. *J Clin Invest* 2003; 111(8): 1221–1230.
  30. Mori H, Kitazawa R, Mizuki S, et al. RANK ligand, RANK, and OPG expression in type II collagen-induced arthritis mouse. *Histochem Cell Biol* 2002; 117(3): 283–292.
  31. Standal T, Seidel C, Hjertner Ø, et al. Osteoprotegerin is bound, internalized, and degraded by multiple myeloma cells. *Blood* 2002; 100(8): 3002–3007.
  32. Michigami T, Ihara-Watanabe M, Yamazaki M, et al. Receptor activator of nuclear factor kappaB ligand (RANKL) is a key molecule of osteoclast formation for bone metastasis in a newly developed model of human neuroblastoma. *Cancer Res* 2001; 61(4): 1637–1644.